FULL PAPER

Dalton
www.rsc.org/dalton

Effect of added metal chelating organosilane on mesoporous titanosilicate formation properties

Michael A. Markowitz,[a] Shalini Jayasundera,[a] Joel B. Miller,[b] John Klaehn,[a] Mark C. Burleigh,[a] Mark S. Spector,[a] Stephen L. Golledge,†[c] David G. Castner[c] and Bruce P. Gaber[a]

[a] *Center for Bio/Molecular Science and Engineering, Code 6900, Naval Research Laboratory, Washington, DC 20375, USA. E-mail: mam@cbmse.nrl.navy.mil; Fax: 1-202-767-9594; Tel: 1-202-404-6072*

[b] *Code 6120, Chemistry Division, Naval Research Laboratory, Washington, DC 20375, USA*

[c] *National ESCA & Surface Analysis Center for Biomedical Problems, Departments of Bioengineering and Chemical Engineering, University of Washington, Seattle, WA 98195-1750, USA*

Received 30th May 2003, Accepted 3rd July 2003
First published as an Advance Article on the web 22nd July 2003

We describe the effects of adding the organosilane n-(trimethoxysilylpropyl)ethylenediaminetriacetic acid (EDATAS) during hydrothermal synthesis on the formation properties of titanium containing SBA-15 mesoporous silica. X-ray photoelectron spectroscopy revealed that the Si/Ti atomic ratio decreased significantly with the addition of the organosilane compared to the non-funtionalized silicates, showing that the EDATAS silicates contained more surface titanium. X-ray powder diffraction and nitrogen gas adsorption analysis revealed that the functionalized titanosilicates were ordered mesoporous materials with narrow pore size distributions with a BJH pore size of 92–96 Å. Solid state CP/MAS NMR experiments demonstrated that addition of EDATAS during hydrothermal synthesis produced a mesoporous silica with 6-coordinated Ti(IV) coordination. Using the same synthesis without the EDATAS, mesoporous silicas with 4-coordinated Ti(IV) were produced.

Introduction

Surfactant template directed synthesis of ordered mesoporous silicas has become a major research field with the potential of producing materials with applications in catalysis and adsorption technologies. There is interest in the preparation of ordered hybrid organic–inorganic mesoporous silicates with tunable surface properties.[1,2] One example of how tuning of surface chemistry can lead to improved material properties involves optimizing the catalytic properties of mesoporous titanosilicates. Recently, ordered, mesoporous titanosilicates functionalized with methyl, vinyl, allyl, 3-chloropropyl, pentyl, and phenyl groups have been prepared using template-directed synthetic methods.[3,4] Surface functionalization with these alkyl and aryl groups increased the hydrophobicity of the titanosilicates resulting in an increase of their efficiency as epoxidation catalysts.

In addition to catalysis,[5] nanoporous titanosilicates are being investigated for their potential as supports for immobilized enzymes,[6–7] and in separation technology.[8] SBA-15 titanosilicates are of particular intertest because of their relatively large pore sizes.[4,9–13] Consequently, we decided to investigate the effects of cocondensation of the organosilane n-(trimethoxysilylpropyl)ethylenediaminetriacetic acid (EDATAS) with titantium(IV) n-butoxide on the formation properties and titanium content of SBA-15 titanosilicates. One component of the ethylenediaminetriacetic acid group is iminodiacetic acid (IDA), a versatile and important metal chelator. The coordination chemistry of IDA has been used successfully to detect and remediate metal ions from solution.[14] In addition, metal ion bound IDA groups are capable of noncovalent bonding interactions with organic compounds and proteins containing accessible amine groups. This capability has been widely exploited in protein separations,[15] development of combinatorial libraries,[16] development of stimulant pancreatic islets,[17] and synthesis of layered polymers.[18] Therefore, surface EDATAS groups would provide a means for further functionalization of titanosilicate surface such as immobilization of proteins or attachment to other surfaces.

The effects of varying the titanium and organosilane content on mesopore structure were investigated using nitrogen gas adsorption, X-ray diffraction (XRD), and X-ray photoelectron spectroscopy (XPS). Because Si–Ti bond formation will have a significant impact on the properties of the final product, we focused our study on a careful examination of the effects of surface functionalization on this process using solid state NMR.

2 Results and discussion

X-ray diffraction analysis

The XRD patterns of the titanium-containing SBA silicates are presented in Fig. 1. In all cases, silicates with large unit cells were formed (Table 1). First and second order diffraction peaks characteristic of ordered SBA-15 materials with hexagonal symmetry were observed. The addition of EDATAS–Ni (2.3%, mol/mol total silica) during synthesis produced silicates with larger d_{100} peaks, but the patterns and unit cells were the same as those observed for the corresponding non-functionalized titanium SBA silicates. The similarity of the unit cells for these silicates suggests that titanium incorporation into these silicates, either within the silicate matrix or on the pore surfaces, did not disrupt their ordered structure.

Nitrogen adsorption

All of the silicates exhibited type IV adsorption isotherms characteristic of mesoporous silica (Fig. 2). A sharp inflection point for each adsorption curve characteristic of capillary condensation was observed indicative of a uniform pore size distribution. The similarity of the inflection point for each of these curves suggests these silicates have similar pore size

† Present address: CAMCOR Surface Analytical Facility, University of Oregon, Eugene, OR 97403, USA.

DOI: 10.1039/b306114k

This journal is © The Royal Society of Chemistry 2003

Table 1 XRD and porosity data for SBA titanium-silicates

Sample	Diffraction peaks	Unit cell[a,b]/Å	BET surface area/$m^2\ g^{-1}$	Pore volume/$cm^3\ g^{-1}$
SBA–Ti10	d_{100}, d_{200}	128	653	1.02
SBA–Ti20	d_{100}, d_{200}	128	549	0.87
SBA–NiETA–Ti10	d_{100}, d_{200}	128	684	1.19
SBA–NiETA–Ti20	d_{100}, d_{200}	128	632	1.07

[a] Calculated based on the 2θ value for d_{100}. [b] Resolution limit is ±4 Å.

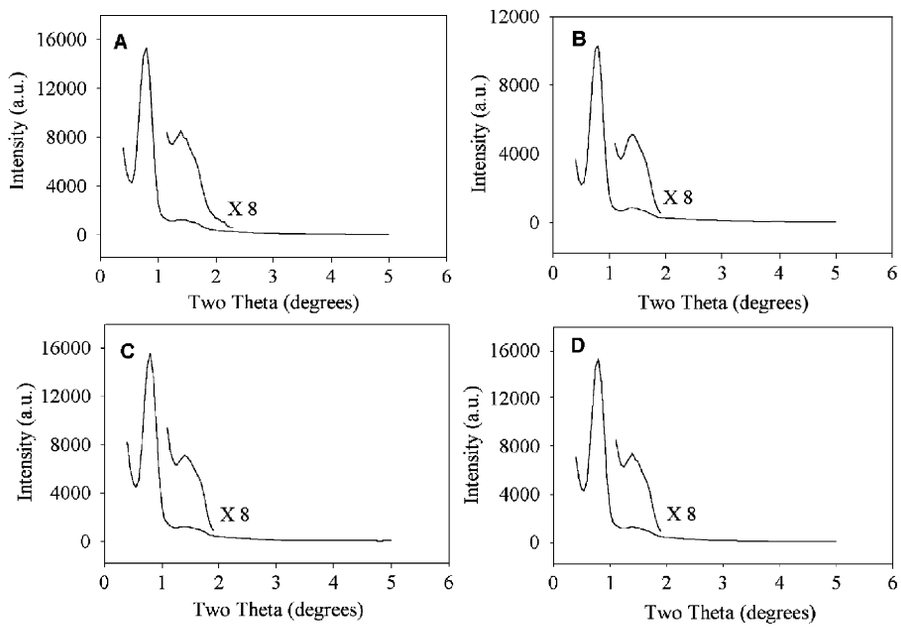

Fig. 1 X-ray powder diffraction data of (A) SBA–Ti10, (B) SBA–Ti20, (C) SBA–NiETA–Ti10, and (D) SBA–NiETA–Ti20.

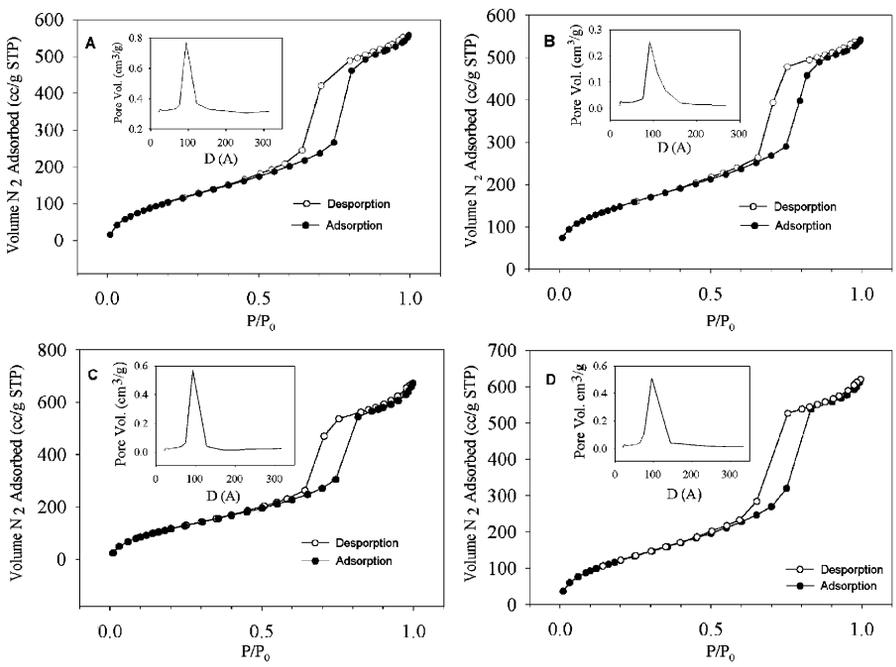

Fig. 2 Nitrogen adsorption-desorption isotherms and BJH pore size distributions (insets) of (A) SBA–Ti10, (B) SBA–Ti20, (C) SBA–NiETA–Ti10, and (D) SBA–NiETA–Ti20.

distributions. Pore size distributions for each silicate are shown as insets for the corresponding gas adsorption plots in Fig. 2. Surface area and porosity data for each silicate are compiled in Table 1. Increasing the amount of added titanium n-butoxide above 10 mol% resulted in a decrease in BET surface area but did not significantly affect pore volume. Increasing the amount of added titanium n-butoxide up to 20 mol% did not appreciably affect the pore size distributions. Peak maxima half-widths were nearly identical. The relatively small peak at higher pore size may result from an increase in macroporosity as the amount of added titanium n-butoxide was increased from 10 to 20 mol%.

The pore size distributions of silicates formed with both titanium n-butoxide and Ni-bound EDATAS added were more sensitive to the amount of added titanium n-butoxide used during synthesis. Increasing the amount of added titanium

Table 2 XPS-measured surface compositions for the SBA titanium-silicates

Sample	Si (atom%)	O (atom%)	C (atom%)	Ti (atom%)	Ni (atom%)	N (atom%)	Si/Ti[b]
SBA–Ti10	28.5 ± 0.5	60.5 ± 1.0	10.8 ± 0.5	0.3 ± 0.1	[a]	[a]	95 (48)
SBA–Ti20	28.2 ± 0.7	61.1 ± 0.4	9.9 ± 0.2	0.8 ± 0.1	[a]	[a]	35 (6.5)
SBA–NiETA	24.5 ± 0.7	58.3 ± 0.9	13.1 ± 0.8	[a]	2.2 ± 0.1	1.2 ± 0.4	[c]
SBA–NiETA–Ti10	25.3 ± 0.5	57.3 ± 0.8	12.5 ± 0.9	0.4 ± 0.1	1.9 ± 0.2	0.9 ± 0.0	63 (30)
SBA–NiETA–Ti20	24.4 ± 0.6	56.2 ± 1.8	14.4 ± 0.9	1.2 ± 0.2	1.5 ± 0.3	0.7 ± 1.2	20 (13)

[a] Element not detected. [b] Bulk ratios in parentheses; calculated from elemental analysis. [c] No titanium detected.

n-butoxide from 5 to 10 to 20% (mol/mol total silica) resulted in increases of peak maxima. In addition, a 45% increase in full width half maximum (FWHM) was observed for SBA–NiETA–Ti20 as compared to SBA–NiETA–Ti10. This increase in FWHM results from an increase in the number of larger diameter pores.

X-ray photoelectron spectroscopy

Powders of the silicates poured onto double-sided tape were characterized by XPS. Table 2 lists data for the elemental composition. As expected, the amount of titanium detected increased with increasing amounts of added titanium n-butoxide. No surface titanium was detected for the silicate formed using 5% added titanium n-butoxide (mol/mol total silica). Low to moderate amounts of surface titanium were detected for silicates formed with 10 and 20% added titanium n-butoxide (mol/mol total silica). Silicates prepared with added EDATAS contained significantly (40–45%) more surface titanium than the corresponding non-functionalized silicates.

Comparison of bulk Si/Ti ratios calculated from elemental analysis (Table 2) to surface Si/Ti ratios determined by XPS revealed that the Ti was not equally distributed throughout the material. Comparing the bulk and surface ratios for the samples formed with 10 mol% added titanium n-butoxide, it is clear that the increased surface titanium detected for the material formed with EDATAS is due to an overall increase in the amount of titanium incorporated into the bulk. However, for the samples formed with 20 mol% added titanium n-butoxide, the increase in surface titanium observed for the material formed with EDATAS can be attributed to the cocondensation of the organosilane with TEOS and the titanium precursor. Specifically, the bulk titanium for SBA–NiETA–Ti20 is approximately half that detected for SBA–Ti20 but the amount of surface titanium is greater for SBA–NiETA–Ti20 and a much higher proportion of the overall titanium content was detected at the surface of SBA–NiETA–Ti20.

Solid-state NMR

Solid-state single pulse (SP) ^{29}Si MAS NMR spectra of ordered mesoporous plain silica and Ti–Si nanoporous material mixed oxides are shown in Fig. 3. The deconvoluted plain silica spectrum (Fig. 3A) displays three resolved peaks at −110, −101, and −92 ppm which can be assigned to $Si(OSi)_n(OH)_{4-n}$ or Q_n structural units within the silica matrix where $n = 4$, 3, and 2, respectively. The increase in the peak intensities by ^{1}H–^{29}Si polarization transfer from the –OH protons to the Si atoms in Q_3 and Q_2 relative to Q_4 in the CP/MAS spectra (Fig. 3A′) confirms the assignment of the Q_n structural units to the respective peak positions in the plain silica spectrum.

The SP ^{29}Si MAS NMR spectrum of the Ti–Si mixed nanoporous silica (SBA–Ti20) is shown in Fig. 3B. In the presence of 20% titanium(IV) n-butoxide the relative amounts of Q_3 (32% to 29%) and Q_2 (13% to 8.6%) decreased while Q_4 (54% to 61%) increased at −111 ppm. The Q_3 and Q_2 peak intensities in the ^{29}Si CP/MAS NMR experiments also decreased relative to Q_4 (Fig. 3B′). The ^{29}Si MAS NMR frequencies of titanosilicates can vary depending on the titanium coordination with the silica. Typical ^{29}Si resonances in four coordinated titanosilicates

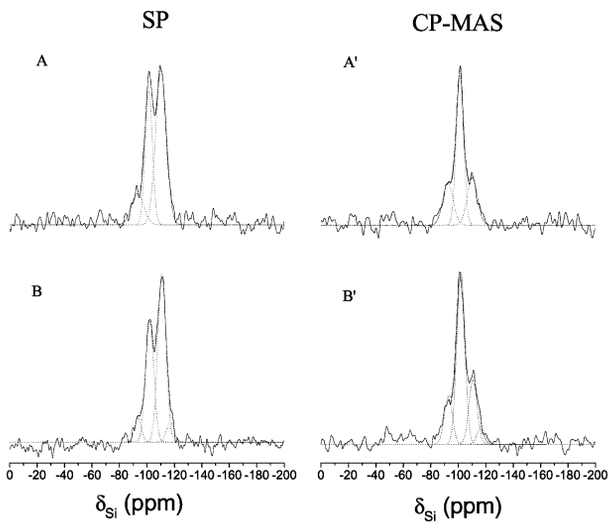

Fig. 3 ^{29}Si MAS NMR spectra of mesoporous silica and Ti–Si mixed nanoporous silica. Single pulse—A. Plain silica, B. SBA–Ti20. CP/MAS—A′. Plain silica, B′. SBA–Ti20.

appear in the range −110 to −116 ppm,[20–21] in five-coordinated titanosilicates a single resonance appear around −107.4 ppm,[22] and in six-coordinated titanosilicates resonances appear in the −90 to −110 ppm range.[23] Hence, the increase in the peak intensity and the small upfield shift (−110 to −111 ppm) of Q_4 in SBA–Ti20 nanoporous silica relative to the plain silica indicates that the titanium is four-coordinated. The shoulder which appears around −116 ppm, which was consistently reproducible, in the SBA–Ti20 spectrum (Fig. 3B) extracted by deconvolution, further points towards a four-coordinated system where this peak can be assigned to Si(3Si, 1Ti) containing Si–O–Ti bonds and the peak at −111 ppm is assigned to Si(4Si, 0Ti).

Solid-state single pulse (SP) ^{29}Si MAS NMR spectra of ordered mesoporous silica made by cocondensation of TEOS and 2.5% (total silica) Ni ion bound ethylenediaminetriacetic acid functionalized triethoxysilane (referred to as SBA–NiETA) and SBA–NiETA–Ti mixed oxides are shown in Fig. 4. The SBA–NiETA spectrum (Fig. 4A) displays a major region centered around −105 ppm with three resolved peaks at −110, −101, and −91 ppm which can be assigned to the Q_n structural units of $Si(OSi)_n(OH)_{4-n}$ within the silica matrix where $n = 4$, 3, and 2, respectively. Another relatively less intense and unresolved region centered around −60 ppm, partially overlapped with the spinning side bands, is assigned to the $RSi(OSi)_{n'}(OH)_{4-n'}$ structural units where $n' = 3$, 2, and 1. The presence of the Ni bound organosilicate groups did not change the chemical shifts or cause significant line broadening in the Q_n structural frequencies indicating minimal affects due to the presence of nickel or EDATAS. Compared to the mesoporous plain SBA silica, the SBA–NiETA silica samples are dominated by Q_4 structural units (approx. 61%). The increase in peak intensities of the Q_3 and Q_2 frequencies in the CP-MAS spectra indicate that approximately 39% of the silica nuclei in the SBA–NiETA samples were attached to –OH groups. This shows that the presence of Ni complexed organo silane functional groups

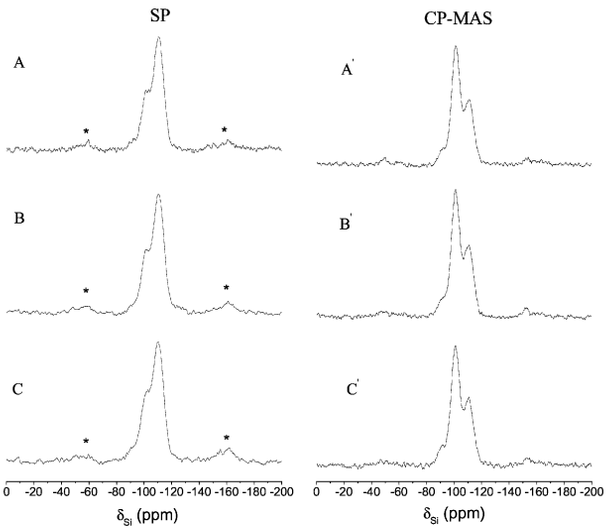

Fig. 4 ^{29}Si MAS NMR spectra of mesoporous SBA–NiETA silica and SBA–NiETA–Ti mixed silica. Single pulse—A. SBA–NiETA, B. SBA–NiETA–Ti10, C. SBA–NiETA–Ti20. CP/MAS—A′. SBA–NiETA, B′. SBA–NiETA–Ti10, C′. SBA–NiETA–Ti20.

caused a higher degree of condensation in SBA–NiETA silica relative to the plain SBA mesoporous silica. Previous studies have shown that condensation in silicates was hampered in NiO–SiO_2 nanocomposites when compared with plain silica.[24] Therefore the increased condensation seen in our samples may indicate that the Ni does not directly interact with the Q_n sites of the silicates (*i.e.* Ni–O–Si interactions), instead only complexes with the organic ligand nuclei in EDATAS. New ^{29}Si-NMR frequencies attributed to Q_n species that can point towards the formation of Ni–O–Si bonds were also not detected.

Ethylenediaminetriacetic acid functionalized triethoxysilane has three carboxyl groups in its structure. The Ni–EDATAS can have either a quinquedentate structure, where two N and three O of EDATAS and one water molecule is coordinated to the metal or a tridentate structure where one carboxyl group is uncomplexed and two water molecules are coordinated to the metal center. A ^{13}C-NMR CP/MAS experiment showed a relatively low intensity broad region of carboxyl resonances strongly suggesting that labile and/or coordinated carboxyl groups with different species were present. Dipolar dephasing CP/MAS experiments[25] in which the ^{1}H decoupling power is interrupted for a period of time after the cross polarization step and before the ^{13}C signal acquisition with high power decoupling was conducted to enhance the carboxyl frequency region. In these experiments the ^{13}C spins with directly bonded protons in a less mobile structure will decay considerably before data acquisition while the ^{13}C spins without any directly bound protons and/or those ^{13}C spins with directly bound protons in a more mobile structure will mostly survive the dipolar dephasing. The ^{13}C-NMR CP/MAS spectrum obtained with 100 μs dipolar dephasing and 3 ms contact time (Fig. 5) exhibits multiple COO– resonances centered around 120 ppm and 160 ppm in the SBA–NiETA silica sample. The upfield chemical shifts are consistent with those C atoms adjacent to ligand donor sites in Ni(II) complexes with ethylenediamines.[26] The downfield shifted resonances (*ca.* 155 ppm) are consistent with those of the free carboxyl groups in a tridentate complex. The ^{29}Si spectra do not provide any evidence for the presence of –COO–Si bonds that might form between the free carboxyl groups and the silicate surface.

The inclusion of up to 20% (total silica) titanium(IV) n-butoxide in the SBA–NiETA silicate did not cause a significant shift of the Q_n peaks. The deconvoluted SP spectra showed that as the titanium content was increased the relative amount of Q_3 sites increased and the Q_4 sites decreased (Fig. 4). The

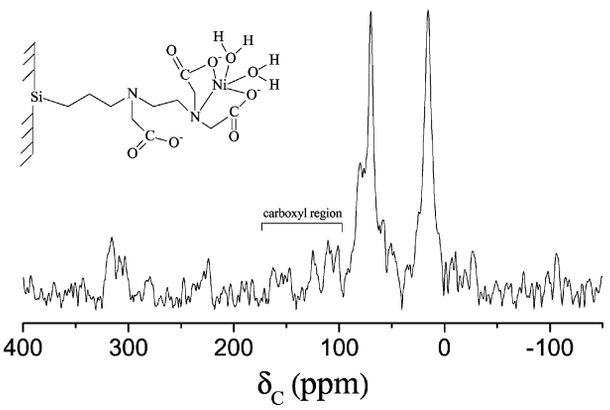

Fig. 5 ^{13}C CP/MAS NMR spectrum of mesoporous SBA–NiETA silica obtained with 100 μs dipolar dephasing.

–OH and –OTi groups show similar effects on the chemical shifts of Si atoms.[27] Hence the peaks at −101 and −92 ppm of Q_3 and Q_2 respectively can have a contribution of the Si–O–Ti groups in the SBA–NiETA–Ti mixed oxides. The CP/MAS experiments, which enhance the peak intensities of Q_3 and Q_2 peaks relative to Q_4 by ^{1}H–^{29}Si polarization from the –OH groups, did not show such behavior in the SBA–NiETA–Ti mixed oxides similar to the SBA–NiETA sample. The SBA–NiETA–Ti mixed oxides showed instead a small increase in the relative intensity of the Q_4 peak. This confirms that the relative increase in the quantity of Q_3 and Q_2 (Fig. 4C) units of the SBA–NiETA–Ti mixed oxides in the SP experiments was not due to Si–O–H bonds but due to the formation of Si–O–Ti bonds. The increase in the amount of Q_3 and Q_2, in the SP experiments, with increasing titanium(IV) n-butoxide content (up to 20%) relative to the SBA–NiETA also indicates that the titanium in these samples is coordinated differently to those in the mesoporous plain silica. The results indicate that the Ti(IV) in the SBA–NiETA–Ti samples are six-coordinated and the Q_3 and Q2 peaks at −101 and −92 ppm can be assigned to contain Si(3Si, 1Ti) and Si(2Si, 2Ti) Si–O–Ti bonds in addition to $Si(OSi)_{3/2}(OH)_{1/2}$.

The ^{13}C CP/MAS spectra of SBA–NiETA–Ti with dipolar dephasing exhibited a considerable decay in all the ^{13}C spins indicating a difference in the T_2 relaxation of the C atoms in the presence of Ti (spectra not shown). The higher degree of dephasing observed in the directly proton bonded ^{13}C spins indicate that the organic ligand groups are less mobile than in the absence of Ti. This study provides no direct evidence on the formation of COO–Ti bonds. However, previous studies on molecular imprinting[28] and surface functionalization[29] have shown carboxylate binding to surface Ti^{4+} ions through unidentate and bidentate configurations. Therefore the marked change in T_2 relaxation and mobility of the C atoms in the Ni–EDATAS may indicate the formation of some COO–Ti bonds with the six-coordinated surface titanium in the SBA–NiETA–Ti silicates. The presence of free carboxyl groups that can bind to Ti^{4+} ions (Fig. 5) and the presence of up to a 45% more surface titanium in the SBA–NiETA–Ti silicates, corresponding to the non-functionalized silicates, may further favor the formation of COO–Ti interactions.

3 Conclusions

Ordered, titanium containing SBA silicates with surface ethylenediaminetriacetic acid groups have been synthesized by direct hydrothermal synthesis. The coordination of Ti(IV) was dependent on the presence or absence of added EDATAS. For titanosilicates prepared without the triethoxyorganosilane, the Ti(IV) was 4-coordinate. The Ti(IV) of the titanosilicates formed with added EDATAS were 6-coordinated. This change in the titanium coordination in the crystalline structure of

titanosilicates can have a major difference in the surface properties of the silicates. Titanosilicates with higher concentrations of silica, which are typically tetrahedral have been shown to be more effective as catalytic surfaces for epoxidation while those with higher concentrations of titanium, which are typically octahedrally coordinated have been shown to be more effective catalytic surfaces in acid catalysed reactions.[30] The surface titanium content of silicates formed with added EDATAS was 40–45% higher than that of the SBA titanosilicates formed without EDATAS.

4 Experimental

Chemicals

n-(Trimethoxysilylpropyl)ethylenediaminetriacetic acid, trisodium salt (EDATAS, 50 wt.% in water) was purchased from Gelest Inc. (Tullytown, PA). Titanium(IV) n-butoxide (98+%) was purchased from Strem Chemicals, Inc. (Newburyport, MA). Pluronic P123 (poly(ethylene oxide)–poly(propylene oxide)–poly(ethylene oxide) triblock copolymer, $PEO_{20}PPO_{70}PEO_{20}$) was obtained from BASF. Hydrochloric acid (HCl, 37% in water) was obtained from Fisher Scientific Co. (Pittsburgh, PA). Tetraethoxysilane (TEOS), 1,3,5-trimethylbenzene (TMB), denatured ethanol, anhydrous dichloromethane, nickel(II) chloride (99.9%), and nickel sulfate (99.9+%) were purchased from Aldrich Chemical Co. (Milwaukee, WI). Water was purified by a Milli-Q filtration system (resistivity >17 MΩ cm).

Synthesis

In a typical preparation for a 5 mol% titanium sample (Ti5–Si), Pluronic P123 (2.0 g) was dissolved in 15 mL of water and 60 g of 2 M HCl while stirring at 37 °C. TEOS (4.25 g) was added with stirring at 37 °C for *ca.* 30 min. Titanium(IV) n-butoxide (0.347 g, 5% mol/mol of total silica) was then added and the mixture was stirred at 37 °C for 20 h. The reaction mixture was then stored in an oven at 80 °C for 24 h. The solid product was subsequently recovered, refluxed in ethanol for *ca.* 10 h, and dried under vacuum. All products were obtained in the form of white finely divided powders.

In a typical preparation for EDATAS functionalized Ti-silicate (SBA–NiETA–Ti), Pluronic P123 (2.0 g) was dissolved in 15 mL of water and 60 g of aq. 2 M HCl solution while stirring at 37 °C. An aqueous solution of pre-chelated EDATAS–Ni (0.94 g, 2.28% mol/mol of total silica) was added while stirring at 37 °C for *ca.* 15 min and then, TEOS (4.25 g) was added. Solutions of the pre-chelated EDATAS–Ni were obtained by vortex mixing of 1 : 1 solutions of 0.54 M $NiCl_2$ and EDATAS in water until a homogeneous blue–green solution was achieved. This mixture was stirred at 37 °C for *ca.* 30 min before the titanium(IV) n-butoxide (0.347 g, 5% mol/mol of total silica) was slowly added. The mixture was stirred at 37 °C for 20 h. The reaction mixture was then stored in an oven at 80 °C for 24 h. The solids were subsequently recovered and all of the products containing nickel were obtained as light blue powders. The silicates were refluxed in ethanol using a 1 M HCl/ethanol solution overnight, and dried under vacuum. Refluxing the material in a 1 M HCl/ethanol solution overnight removed the nickel from the EDATAS. After isolating and drying under vacuum, the resulting functionalized mesoporous titanium-silicates were observed as white powders. Nickel was reabsorbed on these materials using a 1.0×10^{-5} M solution of nickel sulfate when necessary. Typically, 0.2 g of mesoporous material was exposed to 3 mL of nickel sulfate solution for 24 h.

Characterization

X-ray diffraction measurements were made on an Enraf-Nonius FR591 rotating-anode operating at 13 kW. A singly bent graphite monochromator selected Cu Kα radiation and provided in-plane resolution of 0.014 $Å^{-1}$ full-width at half-maximum. Powder samples were placed in 1.0 mm quartz capillary tubes. The unit cell parameter, a, was calculated based on the 2θ value for the d_{100} peak using the following equation: $a = (4/3)^{1/2} d_{100}$.

Gas adsorption experiments were performed using a Micromeritics ASAP 2010 instrument. Nitrogen gas was used as the adsorbate at 77 K. Pore size distributions and total pore volumes were calculated based on BJH (Barrett–Joyner–Halenda) analysis.

X-ray photoelectron spectroscopy (XPS) was performed using a Surface Science Instrument (SSI) SSX-100 spectrometer equipped with a monochromatic, Al Kα X-ray source, hemispherical analyzer, and multi-channel detector. Four spectra were taken for each sample, and the average and standard deviation were calculated from these data. Powders of the samples were poured onto double-sided tape. Spectra were taken from areas containing a relatively large amount of powder; that is, from areas where no tape was visible. A low-energy electron flood gun was used for charge neutralization. Composition data were obtained at pass energy of 150 eV. Bulk Si/Ti ratios were detemined by elemental analysis (Desert Analtics Laboratory, Tucson, AZ).

Solid-state ^{29}Si and ^{13}C NMR experiments were performed at room temperature on a Bruker DMX 500 MHz at a resonance frequency of 99.36 MHz and 125.77 MHz respectively with a 4.0 mm MAS probe. The samples were packed in 4 mm zirconia Bruker rotors fitted with Kel-F end caps for magic angle spinning at 5 kHz for ^{29}Si NMR and 10–12.5 kHz for ^{13}C NMR. A two-pulse phase modulation (TPPM) decoupling[19] was used for proton decoupling in the cross-polarization magic angle spinning (CP/MAS) and single pulse (SP) experiments. A ^{29}Si CP contact time of 3 ms was used for all the samples with up to 6000 scans and 2–5 s recycle delays. Single pulse MAS spectra with high power decoupling were recorded with 5 μs pulses and a recycle delay of 120 s. The ^{29}Si reference was set to external tetrakis(trimethylsilyl)silane at −9.9 ($SiMe_3$) and −135.6 ppm (T = 297 K) with respect to TMS at 0 ppm. A ^{13}C CP contact time of 3 ms was used with up to 40,000 scans and 3 s delays. The ^{13}C reference was set to external tetrakis(trimethylsilyl)silane at 3.5 ppm with respect to TMS at 0 ppm.

Acknowledgements

John Klaehn and Shalini Jayasundera received support as NRC/NRL Postdoctoral Research Associates. The authors thank the Office of Naval Research for providing funding for this work through a Naval Research Laboratory Accelerated Research Initiative. The National ESCA and Surface Analysis Center for Biomedical Problems at the University of Washington is a NIH-supported research center, RR-01296.

References

1 A. Sayari and S. Hamoudi, *Chem. Mater.*, 2001, **13**, 3151.
2 A. Stein, B. J. Melde and R. C. Schroden, *Adv. Mater.*, 2000, **12**, 1403–1419.
3 A. Corma, J. L. Jorda, M. T. Navarro and F. Rey, *Chem. Commun.*, 1998, 1899.
4 A. Bhaumik and T. Tatsumi, *J. Catal.*, 2000, **189**, 31.
5 (*a*) A. Sayari, *Chem. Mater.*, 1996, **8**, 1840; (*b*) R. Murugavel and H. W. Roesky, *Angew. Chem., Int. Ed. Engl.*, 1997, **36**, 477; (*c*) F. S. Xiao, Y. Han, Y. Yu, X. J. Meng, M. Yang and S. Wu, *J. Am. Chem. Soc.*, 2002, **124**, 888; (*d*) K. Chaudhari, R. Bal, D. Srinivas, A. J. Chandwadkar and S. Sivasanker, *Microporous Mesoporous Mater.*, 2001, **50**, 209; (*e*) J. E. Haskouri, S. Cabrera, M. Gutierrez, A. Betran-Porter, D. Betran-Porter, M. D. Marcos and P. Amoros, *J. Chem. Soc., Chem. Commun.*, 2001, 309; (*f*) A. M. Prakesh, H. M. Sung-Suh and L. Kevan, *J. Catal.*, 1998, **178**, 586; (*g*) T. Maschmeyer, F. Rey, G. Sankar and J. M. Thomas, *Nature*, 1995, **378**, 159; (*h*) M. S. Morey, S. O'Brien, S. Schwartz and G. D. Stucky, *Chem. Mater.*, 2000, **12**, 898; (*i*) Z. Luan, E. M. Maes,

P. A. van der Heide, D. Zhao, R. S. Czernuszewicz and L. Kevan, *Chem. Mater.*, 1999, **11**, 3680; (*j*) B. L. Newalkar, J. Olanrewaju and S. Komarneni, *Chem. Mater.*, 2001, **13**, 552; (*k*) Z. Luan, J. Y. Bae and L. Kevan, *Microporous Mesoporous Mater.*, 2001, **48**, 189.
6 F. N. Serralha, J. M. Lopes, F. Lemos, D. Prazeres, M. Aires-Barros, J. Rocha, J. Cabral and F. R. Ribeiro, *React. Kinet. Catal. Lett.*, 2000, **69**, 217.
7 S. S. Rosatto, L. T. Kubato and G. de Oliveira Neto, *Anal. Chim. Acta*, 1999, **390**, 65.
8 (*a*) G. X. S. Zhao, J. L. Lee and P. A. Chia, *Langmuir*, 2003; (*b*) L. Al-Attar, A. Dyer and R. J. Blackburn, *Radioanal. Nucl. Chem.*, 2000, **246**, 451.
9 A. Corma, M. T. Navarro and J. P. Pariente, *J. Chem. Soc, Chem. Commun.*, 1994, 147.
10 P. T. Tanev, M. Chibwe and T. Pinnavaia, *Nature*, 1994, **368**, 321.
11 W. Zhang, M. Froba, J. Wang, P. T. Tanev, J. Wong and T. Pinnavaia, *J. Am. Chem. Soc.*, 1996, **118**, 9164.
12 Y. Han, F. S. Xiao, S. Wu, Y. Sun, X. Meng, D. Li, S. Lin, F. Deng and X. Ai, *J. Phys. Chem. B*, 2001, **105**, 7963.
13 W. H. Zhang, J. Lu, B. Han, M. Li, J. Xiu, P. Ying and C. Li, *Chem. Mater.*, 2002, **14**, 3413.
14 (*a*) R. S. Juang and Y. C. Wang, *Ind. Eng. Chem. Res.*, 2003, **42**, 1948; (*b*) C. C. Wang, C. Y. Chen and C. Y. Chang, *J. Appl. Polym. Sci.*, 2002, **84**, 1353; (*c*) W. Bashir and B. Paul, *J. Chromatogr. A*, 2002, **942**, 73; (*d*) M. Grotti, M. L. Abelmoshi, F. Soggia and R. Frache, *J. Anal. At. Spectrom.*, 2002, **17**, 46; (*e*) I. Moreno-Villoslada, C. Munoz and B. L. Rivas, *Macromol. Rapid Commun.*, 2001, **22**, 1191.
15 (*a*) G. Tishchenko, B. Hodrova, J. Simunek and M. Bleha, *J. Chromatogr. A*, 2003, **983**, 125; (*b*) C. Hidayat, M. Nakajima, M. Takagi and T. Yoshida, *J. Biosci. Bioeng.*, 2003, **95**, 133; (*c*) S. Sharma and G. P. Agarwal, *Sep. Sci. Technol.*, 2002, **37**, 3491; (*d*) Q. Z. Luo, H. F. Zou, X. Z. Xiao, Z. Guo, L. Kong and X. Q. Mao, *J. Chromatogr. A*, 2001, **926**, 255; (*e*) R. S. Pasquinelli, R. E. Shepherd, R. R. Koepsel, A. Zhao and M. M. Ataai, *Biotechnol. Prog.*, 2000, **16**, 86; (*f*) L. Yang, L. Y. Jia, H. F. Zou and Y. K. Zhang, *Biomed. Chromatogr.*, 1999, **13**, 229; (*g*) A. Bossi and P. G. Righetti, *Electrophoresis*, 1997, **18**, 2012; (*h*) J. L. Casey, P. A. Keep, K. A. Chester, L. Robson, R. E. Hawkins and R. H. J. Begent, *J. Immunol. Methods*, 1995, **179**, 105; (*i*) J. Y. Cai and Z. Elrassi, *J. Liq. Chromatogr.*, 1993, **16**, 2007; (*j*) B. H. Chung and F. H. Arnold, *Biotechnol. Lett.*, 1991, **13**, 615; (*k*) Z. Elrassi and C. Horvath, *J. Chromatogr.*, 1986, **359**, 241; (*l*) A. Figueroa, C. Corradini, B. Feibush and B. L. Karger, *J. Chromatogr.*, 1986, **371**, 335.
16 (*a*) J. Goldberg, Q. Jin, Y. Ambroise, S. Satoh, J. Desharnais, K. Capps and D. L. Boger, *J. Am. Chem. Soc.*, 2002, **124**, 544; (*b*) D. L. Boger, J. Goldberg, W. Q. Jiang, W. Y. Chai, P. Ducray, J. K. Lee, R. S. Ozer and C. M. Andersson, *Bioorg. Med. Chem.*, 1998, **6**, 1347; (*c*) D. L. Boger and W. Y. Chai, *Tetrahedron*, 1998, **54**, 3955.
17 A. T. Maghasi, K. T. Schlueter, B. Halsall, W. R. Heineman and H. L. Rodriguez Rilo, *Anal. Biochem.*, 2003, **314**, 38.
18 Q. H. Zhao, H. F. Li and R. B. Fang, *Transition Met. Chem.*, 2003, **28**, 220.
19 A. E. Bennett, C. M. Rienstra, M. Auger, K. V. Lakshmi and R. G. Griffin, *J. Chem. Phys.*, 1995, **103**, 6951.
20 A. Thangaraj, R. Kumar, S. P. Mirajkar and P. J. Ratnasamy, *Catalysis*, 1991, **130**, 1.
21 A. Thangaraj, R. Kumar and S. Sivasanker, *Zeolites*, 1992, **12**, 135.
22 Z. Lin, J. Rocha, P. Brandao, A. Ferreira, A. P. Esculcas, J. D. Pedrosa de Jesus, A. Philippou and M. W. Anderson, *J. Phys. Chem. B*, 1997, **101**, 7114.
23 Y. Liu, H. Du, F. Xiao, G. Zhu and W. Pang, *Chem. Mater.*, 2000, **12**, 665.
24 M. Casu, A. Lai, A. Musinu, G. Piccaluga, S. Solinas, S. Bruni, F. Cariati and E. Beretta, *J. Mater. Sci.*, 2001, **36**, 3731–3735.
25 S. J. Opella and M. H. Frey, *J. Am. Chem. Soc.*, 1979, **101**, 5854.
26 N. A. Matwiyoff, C. E. Strouse and L. O. Morgan, *J. Am. Chem. Soc.*, 1970, **92**, 5224.
27 C. Wies, K. Meise-Gresch, Muller-Warmuth, W. Beier, A. A. Goktas and H. G. Frischat, *Phys. Chem. Glasses*, 1990, **31**, 138.
28 S. W. Lee, I. Ichinose and T. Kunitake, *Langmuir*, 1998, **14**, 2857.
29 C. Mao, H. Li, F. Cui, Q. Feng and C. Ma, *J. Mater. Chem.*, 1999, **9**, 2573.
30 R. J. Davis and Z. Liu, *Chem. Mater.*, 1997, **9**, 2311.